Negative Charge at Amino Acid 149 Is the Molecular Determinant for Substrate Specificity of Lecithin:Cholesterol Acyltransferase for Phosphatidylcholine Containing 20-Carbon *sn*-2 Fatty Acyl Chains†

Yue Zhao, Jingchuan Wang,‡ Abraham K. Gebre, Jeffrey W. Chisholm,§ and John S. Parks*

Department of Pathology, Wake Forest University School of Medicine, Medical Center Boulevard, Winston-Salem, North Carolina 27157

Received August 14, 2003; Revised Manuscript Received September 25, 2003

ABSTRACT: We previously described a point mutation in human LCAT (E to A at residue 149; hE149A) that demonstrated greater activity with phosphatidylcholine (PC) substrate containing 20:4 in the *sn*-2 position compared with the wild-type enzyme [hLCAT; Wang et al. (1997) *J. Biol. Chem. 272*, 280−286], resulting in a human enzyme with the substrate specificity similar to that of rat LCAT. The purpose of the present study was to explore the molecular basis for the role of amino acid 149 in determining fatty acyl substrate specificity. In the first experiment, the reverse mutation in rat LCAT (rA149E) converted substrate specificity of rat LCAT toward that of the human enzyme, demonstrating that the mutation was context independent and reversible. In the second experiment, we found that hE149A compared with hLCAT demonstrated higher activity with PC species containing 20-carbon, but not 18-carbon, *sn*-2 fatty acyl chains. The increased activity of hE149A was due to an increase in apparent V_{max} but not to apparent K_m or LCAT binding to the PC surface. Substitution of different amino acids in the 149 position of hLCAT showed that activation of the enzyme with *sn*-2 20:4 containing PC substrate was only observed when the negative charge at residue 149 was removed. We conclude that the negative charge at amino acid 149 of LCAT is a critical determinant for the specificity of the enzyme for PC containing 18- vs 20-carbon *sn*-2 fatty acyl chains.

Lecithin:cholesterol acyltransferase (LCAT;[1] EC 2.3.1.43) is a plasma glycoprotein that is secreted by the liver into plasma where it catalyzes the synthesis of cholesteryl esters (CEs) (*1*). Three-fourths of the cholesterol in plasma lipoproteins is in the esterified form, and it is believed that most of the CE in human plasma originates from the LCAT reaction (*2*). During the LCAT reaction, a fatty acid is cleaved from the *sn*-2 position of phophatidylcholine (PC) and transesterified to the free hydroxyl group of cholesterol to generate CE (*3*). The reaction is activated by apolipoproteins, in particular, apolipoprotein A-I (apoA-I), the major apolipoprotein of high-density lipoprotein (HDL) (*4*). LCAT is essential for the maturation of nascent HDL and helps to maintain the physiologic composition and shape of plasma lipoproteins (*5*−*7*). In addition, the esterification reaction decreases the amount of free cholesterol in the surface monolayer of plasma lipoproteins as the more hydrophobic CE product is less soluble in the surface and partitions into the core of the HDL particle (*6*). This physical−chemical change in cholesterol is believed to explain the role of LCAT in reverse cholesterol transport, a process in which excess free cholesterol in peripheral tissues is taken up by HDL particles, esterified by LCAT, and transported to the liver for uptake by the scavenger receptor class B, type I (*5*).

The enzymatic activity of LCAT appears to primarily be determined by the type of PC substrate it encounters in lipoprotein particles. Using synthetic recombinant HDL (rHDL) substrate particles composed of different PC species, Jonas et al. (*8*) demonstrated that the cholesterol esterification activity of purified human LCAT varied 100-fold among rHDL. The source of this variability in activity appears to be related to binding of monomeric PC substrate molecules to the active site of the enzyme. Experiments in which the surface of the rHDL was composed of 90% of an inert ether analogue of PC and 10% of the diacyl-PC substrate demonstrated a rank ordering of PC reactivity that was similar to that observed for rHDL particle surfaces containing 100% PC (*9*, *10*). This latter result suggests that, although PC fatty acyl composition affects physical properties of the

† This work was supported by National Institutes of Health Grants HL-54176 and HL-49373 (J.S.P.) and American Heart Association Grants 0212123U (Y.Z.), 95041130 (J.W.), and 9804829U (J.W.C.).

* To whom correspondence should be addressed. E-mail: jparks@wfubmc.edu.

‡ Present address: Department of Pathology, University of Florida Health Science Center/Jacksonville Campus, 655 West 8th St., Jacksonville, FL 32209.

§ Present address: Discovery Research, CV Therapeutics Inc., 3172 Porter Drive, Palo Alto, CA 94304.

[1] Abbreviations: LCAT, lecithin:cholesterol acyltransferase; PC, phosphatidylcholine; hE149A, human LCAT with E for A substitution at amino acid 149; hLCAT, human wild-type LCAT; rA149E, rat LCAT with A for E substitution at amino acid 149; CEs, cholesteryl esters; apoA-I, apolipoprotein A-I; HDL, high-density lipoprotein; rHDL, recombinant HDL; POPC, 1-palmitoyl-2-oleoyl-*sn*-glycero-3-phosphocholine; PAPC, 1-palmitoyl-2-arachidonoyl-*sn*-glycero-3-phosphocholine; PLA_2, phopholipase A_2; PCR, polymerase chain reaction; rLCAT, rat wild-type LCAT; ELISA, enzyme-linked immunosorbent assay; CHO, Chinese hamster ovary; BCA, bicinchoninic acid; BCIP, 5-bromo-4-chloro-3-indolyl phosphate.

10.1021/bi035460u CCC: $25.00
Published on Web 10/31/2003

rHDL particle surface, it is the monomeric PC conformation that has the greatest impact on determining the activity of the enzyme.

The primary sequence of LCAT is highly conserved across the many species that have been analyzed (*11*). Despite an 87% primary sequence identity between the rat and human LCAT sequence, there is a marked difference in activity of these enzymes with different PC fatty acyl substrates. For example, human LCAT shows higher CE formation activity when reacted with PC substrate molecules containing 18:1 and 18:2 in the *sn*-2 position, whereas the rat enzyme demonstrates higher activity with PC species containing longer chain (>18-carbon chain length) fatty acids in the *sn*-2 position (*12*−*15*). The species difference in LCAT activity can also be observed at the phospholipase A_2 (PLA_2) step of the reaction as release of free fatty acid from the *sn*-2 position of PC substrate when cholesterol is not included in the rHDL substrate particles (*16*). We have referred to this activity difference in rat and human LCAT as the "reactivity" or "specificity" of the enzyme, since differences in activity of these two enzymes can be observed with PC substrates that contain a mixture of 18 and longer fatty acyl chains in the *sn*-2 position (*15*, *17*). However, the molecular explanation for the difference in PC substrate specificity between the human and rat LCAT enzymes is unknown.

In an effort to identify the regions of primary sequence in LCAT that were involved in PC fatty acyl specificity, we performed a mutagenesis study in which different regions of the human LCAT protein were mutated to the corresponding rat sequence (*16*). The mutant LCAT enzymes were expressed and tested for their ability to react with PC substrate molecules containing 1-palmitoyl-2-oleoyl-*sn*-glycero-3-phophocholine (POPC) or 1-palmitoyl-2-arachidonoyl-*sn*-glycero-3-phophocholine (PAPC). We found that a single amino acid substitution at position 149 of human LCAT (glutamic acid replaced by alanine; E149A) was sufficient to convert the PC fatty acyl specificity of human LCAT to that of rat LCAT. Thus, the E149A mutant form of LCAT was more reactive with rHDL containing PAPC compared to rHDL containing POPC, similar to the wild-type rat enzyme, whereas the human enzyme was more reactive with POPC compared with PAPC. Furthermore, the substrate specificity was observed for both CE formation and the PLA_2 step of the reaction. These results suggested that this region of LCAT was critical in determining the substrate specificity of the enzyme and that it most likely resided near the active site of the enzyme. The subsequent publication of a three-dimensional model of LCAT supported this hypothesis and suggested that amino acid 149 resided in a flexible loop region close to the active site serine 181 of human LCAT (*18*).

Although we have documented that amino acid 149 is critical in determining the activity of LCAT with PC substrates containing different *sn*-2 fatty acyl compositions, the molecular explanation of such a striking alteration in enzyme specificity is unknown. There are several unanswered questions that are the focus of the present study. First, we wished to determine whether the change in LCAT substrate specificity that occurred with the E149A mutation was specific for the human enzyme (i.e., context specific) or was this region of LCAT important in substrate specificity in rat LCAT. In other words, would the opposite mutation (alanine to glutamic acid; A149E) in rat LCAT restore the fatty acyl specificity of the human enzyme? Second, we wished to determine whether the PC substrate specificity observed for the E149A mutant form of human LCAT was specific for POPC and PAPC or was it a more general specificity that depended on *sn*-2 fatty acyl chain length and number and position of double bonds along the fatty acyl chain. Finally, we were interested in the molecular properties (i.e., charge or hydrophobicity) of the amino acid at position 149 that determined the PC fatty acyl specificity of the enzyme.

EXPERIMENTAL PROCEDURES

PCR Site-Directed Mutagenesis. The mutations at position 149 of human LCAT were generated by a megaprimer PCR site-directed mutagenesis procedure (*16*). The first round of PCR included a 5′ sense primer (5′-CTTCT TCACC ATCTG GCTGG-3′) about 300 bp upstream of the mutation site and a mutagenic antisense primer with the wild-type LCAT cDNA as template. In the second round of PCR, a 3′ antisense primer (5′-CTCGG TGCTG CGGGT CGCCA-3′) about 600 bp downstream from the mutation site and the purified PCR product (megaprimer) from the first round were used. The sequences of the mutagenic primers were as follows: E149D, 5′-GCCGG GGTCC AGCCG CCAGT CATAG G-3′; E149K, 5′-GCCGG GCTTC AGCCG CCAGT CATAG G-3′; E149L, 5′-GCCGG GCAGC AGCCG CCAGT CATAG G-3′; E149Q, 5′-GCCGG GTTGC AGCCG CCAGT CATAG G-3′; and rA149E, 5′-CTGGC GGGGT TCCAG ACGCC AG-3′. Primers for the generation of the E149A LCAT mutant have been reported (*16*). The A149E mutation of the rat cDNA (rA149E) was constructed using a 5′ sense primer (5′-ACCGG CTAGA AGCCA AGCTG-3′) about 350 bp upstream of the mutation site of rat LCAT cDNA and a 3′ antisense primer (5′-CCAGC TAGTA GGTCA CGAGA CTG-3′) about 470 bp downstream from the mutation site. The sequence for rat LCAT cDNA (GenBank accession number U62803) used in this study has been published (*19*). The final ∼900 bp PCR product for LCAT mutants in the human background and the 820 bp PCR product for rA149E mutant were purified using a PCR minicolumn (Qiagen), digested with *Kpn*I and *Pst*I restriction enzymes for human LCAT constucts or *Nhe*I and *Bam*HI for rat LCAT constructs, and ligated into the pCMV5 human and rat LCAT plasmid restricted with the same two enzymes, respectively. The correct sequence of the mutant constructs between the two restriction sites was confirmed by dideoxy sequencing.

In Vitro Expression and Mass Quantification of hLCAT and Mutants. The hLCAT, hE149A, rLCAT, and rA149E cDNAs were transiently transfected, using a DEAE-dextran method into COS-1 cells, as described previously (*16*). After the transfection, the cells were incubated with serum-free medium for an additional 72 h at 37 °C. The medium was collected, centrifuged at 500*g* for 10 min, and immediately frozen at −70 °C until assays were performed. In one experiment (Figure 2), the medium containing human LCAT or hE149A was assayed in triplicate for LCAT mass using an ELISA procedure and chicken anti-human LCAT antiserum as reported previously (*16*).

Cloning, Expression, and Purification of Carboxy-Terminal Histidine 6 Human LCAT (hLCATh6) and Mutants. The human LCAT cDNA was used as template for PCR

mutagenesis as previously described (*20*), using a 5′ complementary forward primer and a 3′ reverse primer designed to append the sequence for six carboxy-terminal histidine residues, a stop codon, and a 3′ *Bam*HI restriction site. The 500 bp PCR product was digested with *Pst*I and *Bam*HI restriction enzymes and ligated into the pCMV5 human LCAT plasmid, which had been restricted with the same two enzymes and purified. The sequence of the region containing the PCR-generated insert was confirmed to be correct by dideoxy sequencing of the hLCATh6 cDNA, after which the plasmid was digested with *Pst*I and *Bam*HI and the 500 bp fragment containing the 3′ histidine tag was gel purified. The purified 500 bp *Pst*I/*Bam*HI fragment encoding the histidine tag was then ligated into each of the pCMV5 LCAT mutant plasmids that had been previously restricted with *Pst*I and *Bam*HI and gel purified.

Generation of Chinese hamster ovary (CHO) stable cell lines that express hLCATh6 and purification of hLCATh6 have been described previously (*20*). Briefly, the CHO cells were cotransfected with hLCATh6 plasmid or mutant plasmid and pSV3-neo by using FuGENE 6 (Roche). The transfected cells were cultured in medium containing 700 μg/mL G418 (Geneticin, Gibco-BRL) for up to 2 weeks. Surviving colonies were selected and screened by measuring the LCAT activity secreted into the medium, normalized to cell protein. The cell lines were maintained under continuous selection using 700 μg/mL G418 in DMEM/F12 (Mediatech), 10% heat-inactivated fetal bovine serum, 0.01% penicillin−streptomycin, 2 mM L-glutamine, and vitamins. For LCAT expression studies, the cells were switched to PFX-CHO (Hyclone) serum-free complete growth medium and incubated for 72 h. To boost expression, sodium butyrate (10 mM final concentration) was added to the medium for the last 48 h. Talon cobalt metal affinity resin (Clontech) was incubated with the collected medium for 2 h at 4 °C to bind the His_6-tagged wild-type or mutant LCAT enzymes and then transferred to a small column (Bio-Rad). Recombinant His_6-tagged LCAT enzyme was eluted from the column with wash buffer containing 50 mM imidazole (Fisher) and 10% glycerol (Fisher) and immediately frozen at −70 °C. Secondary structural analysis of hLCATh6 and hE149Ah6 as performed by circular dichroism spectroscopy was described previously (*21*). The secondary structural content was estimated with Neural, a network approach using the CDNN software (*22*).

Mass Quantification of CHO hLCATh6 and Mutants. The protein in the purified His_6-tagged wild-type and mutant hLCAT preparation was measured using modified detergent-compatible bicinchoninic acid (BCA) protein assay (Pierce). Because 50 mM imidazole interfered with the standard BCA assay, the LCAT protein was precipitated by trichloroacetic acid (TCA) (6% final concentration) in the presence of deoxycholate (1.25% final concentration). The protein precipitate was pelleted by centrifugation at 1500*g* for 30 min and then was incubated with 2 mL of BCA working reagent. An equivalent amount of imidazole and glycerol was added to the BCA standards, and they were processed in the same way as the LCAT proteins.

The amount of purified LCAT mutant proteins was also analyzed by Western blots. The same amount of protein from each purified preparation (based on the modified BCA assay) was analyzed in duplicate by 7.5% SDS−PAGE gels. The protein bands were transferred to nitrocellulose membranes that were then exposed to primary rabbit anti-hLCATh6 antibody (1:1000; Novus Biologicals, Inc.), followed by goat anti-rabbit IgG conjugated to alkaline phosphatase (Sigma). The protein bands were visualized by enzymatic reaction using BCIP (5-bromo-4-chloro-3-indolyl phosphate; Promega) and NBT (nitroblue tetrazolium; Promega) as substrates. The membranes were scanned, and the intensities of bands were measured by densitometry. The intensities of the mutant hLCATh6 were expressed as the percentage relative to wild-type hLCATh6, because some mutants were more susceptible to proteolysis than wild-type LCAT. The final concentration of the mutants was calculated from the percentage of intensity relative to wild type.

Recombinant HDL Synthesis and LCAT Assay. rHDL used as substrate particles for CE formation by LCAT were synthesized by a cholate dialysis procedure using synthetic PC species as detailed in a previous publication (*10*). rHDL were made with purified human plasma apoA-I, cholesterol, and PC in a starting molar ratio of 1:5:80, with a trace amount of [^{3}H]cholesterol (50000 dpm/ μg of cholesterol). rHDL were made to measure the PLA_2 step of the LCAT reaction by omitting the cholesterol and using POPC or PAPC radiolabeled in the *sn*-2 position as described previously (*16*). Routine LCAT assays were performed in duplicate in 0.5 mL of buffer containing rHDL substrate (1 or 6.2 μM cholesterol as indicated in the figure legends) using transiently transfected COS cell medium or purified LCAT as the enzyme source as described previously (*23*, *24*). The incubation time was adjusted to keep the CE formation under 20% to prevent product inhibition. After incubation, the lipids were extracted, and the radiolabeled free cholesterol and esterified cholesterol were separated by TLC using a neutral solvent system and quantified by scintillation counting. LCAT activity was expressed as nanomoles of CE formed per microgram of LCAT per hour.

For kinetic assay, LCAT activity was measured in duplicate as a function of increasing concentration of rHDL (0.26−6.2 μM cholesterol) as described above, using purified LCAT as the enzyme source. Apparent V_{max} and K_m values for cholesterol esterification were determined from a nonlinear least-squares regression analysis of the Michaelis−Menten equation [activity = (V_{max} × μM cholesterol)/(K_m + μM cholesterol) using a single rectangular hyperbole function in Sigma Plot (Jandel Scientific).

LCAT Binding Assay. rHDL were prepared with POPC or PAPC and purified to apparent homogeneity using FPLC as described previously (*21*). rHDL in PBS were mixed with 10 mg/mL EZ-Link Sulfo LC biotin reagent (Pierce, Rockford, IL) at an apoA-I:biotin reagent mass ratio of 2.7. The mixture was incubated at 4 °C for 1 h, after which time the reaction was adjusted to 0.05 M glycine with a 0.5 M glycine stock solution to quench the reaction. Biotinylated rHDL were extensively dialyzed against PBS to remove glycine and unreacted biotin reagent and repurified by Superdex chromatography. rHDL contained 1−1.5 biotin substitutions per particle, as determined by the avidin−2-(4′-hydroxyazobenzene)benzoic acid assay as described in the manufacturer's instructions (*25*).

rHDL were incubated with streptavidin-substituted Sepharose (Pierce, Rockford, IL, or Amersham-Pharmacia) at 80 μg of cholesterol/mL of a 50:50 bead slurry and washed three

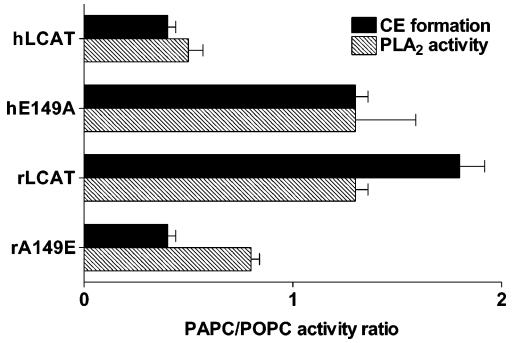

FIGURE 1: PAPC/POPC activity ratio for cholesterol esterification (solid bars) and PLA_2 activity (striped bars). COS cells were transiently transfected with human LCAT (hLCAT), rat LCAT (rLCAT), or mutant cDNA constructs (hE149A, rA149E). The media were assayed for cholesterol esterification and PLA_2 activity using subsaturating concentrations of rHDL containing POPC and PAPC as described in the Experimental Procedures section (1 μM cholesterol for cholesterol esterification or 16.6 μM PC for PLA_2 activity). The activity ratio is expressed as the mean ± SEM of three separate transfections.

times with PBS. Phospholipid on the beads was measured enzymatically (Wako), and the final immobilized rHDL preparation was adjusted with Sepharose G-25 to yield 1 μg of rHDL phospholipid/μL of a 50:50 bead slurry.

Recombinant hLCATh6 was radiolabeled by incubating CHO cells expressing hLCATh6 or hE149Ah6 with [^{35}S]Cys/Met, followed by LCAT purification from the medium as described previously (*20*). The specific activity of the LCAT preparations averaged 5000 cpm/μg of protein. Binding reactions were performed in duplicate using either immobilized HDL or a mock preparation of strepavidin-substituted beads and Sepharose G-25. Binding was performed using 0−20 μg of the radiolabeled LCAT preparation and 20 μg of biotinylated rHDL in a 100 μL reaction containing 1% fatty acid free BSA (final concentration, Sigma). The mixture was incubated for 0.5 h at 4 °C, and the beads were washed three times with 100 μL of TBS containing 1% BSA (fatty acid free). Bound LCAT was determined after liquid scintillation counting of the beads and adjusting for nonspecific binding to the control beads. Binding constants were determined from Eadie−Scatchard plots of the data; B_{max} was expressed in terms of apoA-I, based on the known phospholipid to apoAI ratio for the rHDL preparation.

RESULTS

We have previously shown that when E149 of human LCAT was mutated to an alanine residue, which is present in rat LCAT at position 149 (hE149A), the fatty acyl specificity of the human enzyme was converted toward that of rat LCAT (*16*). The A149E mutant (rA149E) was generated in rat LCAT to determine whether the reverse mutation in the rat background would result in the fatty acyl specificity of human LCAT. cDNA constructs were transiently expressed in COS cells, and the media were assayed for CE formation using rHDL containing POPC or PAPC. The PLA_2 activity was also measured using POPC or PAPC rHDL, which was cholesterol free and contained radiolabeled PC. Figure 1 shows the PAPC/POPC activity ratios for human LCAT (hLCAT), hE149A, rat LCAT (rLCAT), and rA149E. The human wild-type LCAT was less active with PAPC than POPC containing rHDL as demonstrated by a PAPC/POPC activity ratio of 0.4 ± 0.04 for cholesterol esterification and 0.5 ± 0.07 for PLA_2 activity. The opposite activity trend was observed for rat LCAT, with PAPC/POPC activity ratios of 1.8 ± 0.12 and 1.3 ± 0.06, respectively. The hE149A mutant resulted in an activity ratio similar to that of rat LCAT as described previously (*16*). When the reverse mutation was made in rat LCAT (rA149E), the activity ratio dropped to values similar to that of human wild-type LCAT (0.4 ± 0.04 for cholesterol esterification and 0.8 ± 0.07 for PLA_2 activity). Thus, a single amino acid change, independent of LCAT species background, was sufficient to confer PC substrate fatty acyl preference for both cholesterol esterification and PLA_2 activity.

The increased PAPC/POPC activity ratio of the hE149A LCAT mutant was due predominantly to an increase in activity with PAPC (*16*). We were interested in determining whether the increase in activity depended on *sn*-2 fatty acyl chain length, the number and position of the double bonds, or the conformation of double bonds along the fatty acyl chains. PC species were synthesized from 1-palmitoyllyso-PC and various fatty acids, purified, characterized as described (*21*), and used to make rHDL substrate particles to measure the cholesterol esterification by LCAT. Medium from COS cells transfected with hLCAT or hE149A cDNA was used as the source of enzyme. The specific activity of cholesterol esterification for hLCAT and hE149A with rHDL containing different 18- and 20-carbon *sn*-2 fatty acyl chains is shown in Figure 2. There was a 13-fold variation in reactivity exhibited among the *sn*-2 18-carbon PC substrates, with no apparent difference in activity between hLCAT and hE149A (Figure 2A), except perhaps for 18:3 (*9*, *12*, *15*). However, the specific activity of hE149A with different *sn*-2 20-carbon PC substrates was uniformly greater than that of hLCAT (Figure 2B). We have also observed greater activity of hE149A relative to hLCAT with PC containing 22:6 $n-3$ in the *sn*-2 position (data not shown). These results demonstrate that, despite the effect of PC *sn*-2 fatty acyl chain composition on LCAT activity, the hE149A mutant is more reactive with *sn*-2 20-carbon, but not 18-carbon, fatty acyl chains compared to hLCAT.

To better understand the molecular mechanism by which the hE149A mutation selectively activates LCAT toward 20-carbon *sn*-2 fatty acyl PC substrates, we performed enzyme kinetic and rHDL binding studies using hE149A and hLCAT. Since all *sn*-2 18-carbon PC species were equally reactive with both enzymes and all *sn*-2 20-carbon PC species were more reactive with hE149A compared to hLCAT (Figure 2), we continued to use rHDL particles containing POPC or PAPC to discriminate the activity differences between hE149A and hLCAT. Recombinant human and mutant LCAT with a carboxy-terminal histidine tag (hLCATh6 and hE149Ah6) were stably expressed in CHO cells and purified as the enzyme source. A previous study showed that the carboxy-terminal histidine-tagged version of the wild-type enzyme had kinetic properties similar to that of human LCAT purified from plasma (*20*). Substrate saturation curves (Figure 3) for CE formation by hLCATh6 and hE149Ah6 were performed with rHDL containing PAPC or POPC and demonstrated distinct differences in kinetic behavior. The apparent maximal velocity (apparent V_{max}) and apparent K_m values derived from the substrate saturation curves in Figure

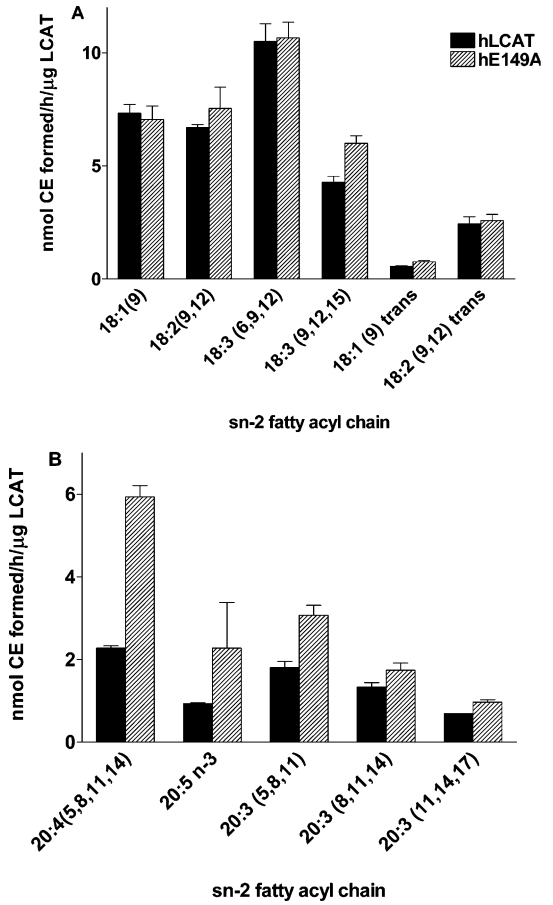

FIGURE 2: Specific activity of hLCAT and hE149A with *sn*-1 16:0 PC substrates containing different 18-carbon (panel A) or 20-carbon (panel B) *sn*-2 fatty acyl chains. Subsaturating concentrations of rHDL containing the indicated PC, [^{3}H]cholesterol, and apoA-I (1 μM cholesterol) were reacted with media from COS cells transfected with hLCAT or hE149A cDNA as the enzyme source. The PC species are designated by the *sn*-2 carbon chain length, the number of double bonds, and the position of the double bonds from the carboxyl group. The cholesterol esterification rate was normalized for the amount of LCAT protein in the media, determined by ELISA. Values are expressed as the mean ± SEM for three separate transfections.

3 are presented in Table 1, along with the constants for LCAT binding to rHDL particles. The apparent V_{max} values, which are thought to reflect the reactivity of LCAT for its molecular substrates (*26*), were significantly higher for hE149Ah6 reacting with PAPC compared to hLCATh6 (31.3 ± 1.6 vs 23.9 ± 1.4 nmol h^{-1} μg^{-1}, respectively, $P < 0.005$), whereas it was significantly lower with POPC (24.4 ± 1.1 vs 37.3 ± 1.9 nmol h^{-1} μg^{-1}, respectively, $P < 0.001$). The PAPC/POPC activity ratio at V_{max} was 1.28 for hE149Ah6 and 0.64 for hLCATh6, similar to values obtained at subsaturating substrate concentrations (Figure 1). In contrast to the apparent V_{max} values, the apparent K_m values were similar for both LCAT enzymes and PC substrate types. LCAT binding to rHDL was also measured using ^{35}S-radiolabeled purified LCAT preparations. The values for B_{max} and K_d were similar for both enzymes and with both POPC and PAPC rHDL particles. Thus, the rHDL particle binding assay agreed well with the apparent K_m data and suggested that the increased activity of hE149Ah6 for PAPC rHDL was not due to the enhanced LCAT binding affinity but rather to an increased apparent V_{max}.

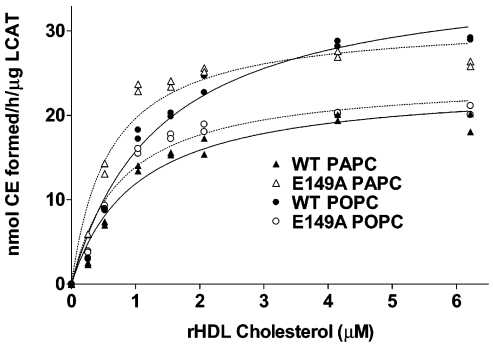

FIGURE 3: Substrate saturation curves for rHDL particles containing POPC or PAPC. rHDL were incubated with purified hLCATh6 and hE149Ah6 to measure CE formation as described in the Experimental Procedures section. Data points represent duplicate determinations for each curve. The line of the best fit, determined by nonlinear least-squares analysis, is also shown for each data set.

To determine whether a mutation at residue 149 of hLCAT induced a significant alteration in secondary structure of the enzyme, we performed a circular dichroism study with one preparation each of hLCATh6 and hE149Ah6. The spectra were analyzed from 190 to 260 nm, and hLCATh6 was predicted to have 24.6% α helix, 22.1% antiparallel β sheet, 8.0% parallel β sheet, 17.9% β turn, and 28.5% random coil. The α helix and β turn content agreed closely with published data from Jin et al. (*27*), but our hLCATh6 preparation contained less β sheet (30.1% vs 42%) and more random coil (28.5% vs 15%) structure than that reported by Jin et al. hE149Ah6 was estimated to have 24.8% α helix, 24.3% antiparallel β sheet, 8.2% parallel β sheet, 17.7% β turn, and 27.1% random coil. On the basis of these results, there was no apparent difference in the secondary structure between hLCATh6 and hE149Ah6.

To systematically investigate the effect of different amino acids at position 149 of LCAT on activity and fatty acyl specificity, a series of substitution mutants were made. hE149Dh6 retains the negative charge but has reduced side chain size. hE149Qh6 has a polar uncharged side chain similar in size to the glutamic acid. hE149Ah6 and hE149Lh6 are nonpolar, uncharged hydrophobic substitutions with different side chain sizes. Finally, hE149K contains the positive charge at position 149. The mutant enzymes were stably expressed and purified along with hLCATh6 as described previously (*20*). LCAT CE formation was measured using rHDL at saturating cholesterol substrate concentration (6.2 μM cholesterol). The results are shown in Figure 4. Panel A shows the cholesterol esterifying activity of each mutant LCAT with rHDL containing PAPC or POPC. Several of the mutant LCATs (i.e., hE149Qh6 and hE149Kh6) had a substantial decrease in specific activity with both rHDL substrate particles. To normalize the differences in specific activity of the mutant enzymes and to address the effect of amino acid 149 substitutions on reactivity of the enzyme with PAPC, a ratio of specific activity was calculated and plotted (Figure 4B). Despite a severalfold range in specific activity among the enzyme preparations, all mutant LCAT proteins demonstrated increased reactivity with PAPC compared to POPC rHDL, except the wild-type enzyme (E) and the E149D mutant enzyme. Thus, only the LCAT proteins that retained a negatively charged amino acid at residue 149 were more reactive with POPC than PAPC, whereas several amino

Table 1: Kinetic and Binding Constants for LCAT with rHDL Containing POPC or PAPC[a]

	app V_{max} (nmol of CE h^{-1} μg^{-1})		app K_m (μM Chol)		B_{max} (LCAT/apoA-I)		K_d (μM LCAT)	
protein	PAPC	POPC	PAPC	POPC	PAPC	POPC	PAPC	POPC
hLCAT	23.9 ± 1.4	37.3 ± 1.9	1.01 ± 0.18	1.37 ± 0.19	0.8 ± 0.2	0.8 ± 0.2	5.8 ± 2.0	4.7 ± 0.8
hE149A	31.3 ± 1.6[b]	24.4 ± 1.1[c]	0.59 ± 0.11	0.76 ± 0.12	0.65 ± 0.1	1.0 ± 0.5	8.1 ± 0.5	11.0 ± 6.0

[a] The human LCAT and E149A with six carboxy-terminal histidine residues were purified from stably transfected CHO cells. The protein concentration of the purified preparations was measured by a modified BCA assay and Western blots as described in the Experimental Procedures section. The apparent V_{max} and apparent K_m were determined from the substrate saturation curves shown in Figure 3 by nonlinear regression analysis using the single rectangular hyperbole function in Sigma Plot (Jandel Scientific). The B_{max} and K_d were determined from Eadie−Scatchard plots. Results are representative of two or more experiments and are presented as parameter ± standard error. Statistical differences between hLCAT and hE149A were determined by Student's *t*-test. [b] $P < 0.002$. [c] $P < 0.001$.

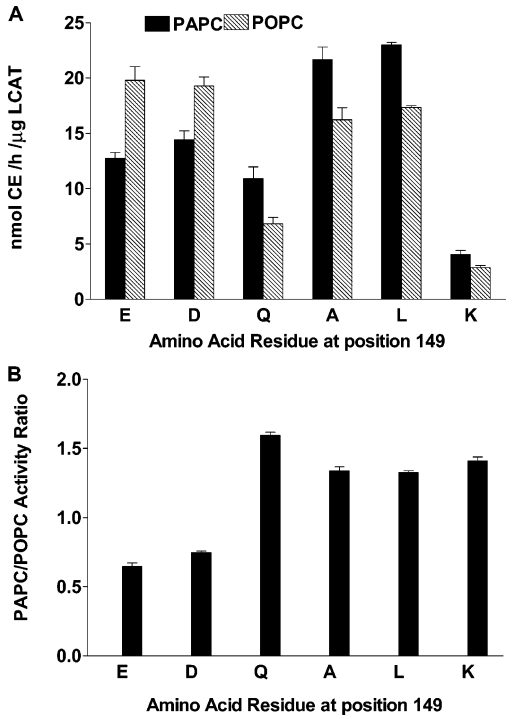

FIGURE 4: Effect of amino acid substitutions at residue 149 on cholesterol esterification by LCAT. E149 was substituted with D, Q, A, L, and K. LCAT incubations were performed with saturating substrate concentrations (6.2 μM cholesterol) in duplicate as described in the Experimental Procedures section. The LCAT source was purified histidine-tagged human LCAT or mutants. The data represent the mean ± SEM of three different purifications for each LCAT protein. Panel A: Specific activity of LCAT proteins with PAPC rHDL (solid bars) and POPC rHDL (striped bars). Panel B: PAPC/ POPC activity ratio.

acid substitutions that removed the negative charge at residue 149 resulted in increased reactivity with PAPC.

Enzymatic kinetic studies were performed with all five mutant forms of LCAT to determine whether the increased reactivity with PAPC that occurred with the loss of a negative charge at amino acid 149 was the result of an increase in apparent V_{max}, as was observed for hE149A (Table 1). The results are summarized in Table 2. The apparent V_{max} values obtained for all of the mutants reacted with rHDL containing PAPC or POPC agreed reasonably well with their specific activities using saturating substrate concentration in Figure 3. The results show that the main effect of each amino acid substitution at position 149 was on the apparent V_{max} and not the apparent K_m. This can best be observed by analysis of the PAPC/POPC ratios of apparent V_{max}, which showed that the ratio was increased, compared to wild-type LCAT, with substitutions at position 149 that resulted in a loss of negative charge.

DISCUSSION

Human and nonhuman primate LCAT are more active with PC substrates containing *sn*-2 18:1 or 18:2 fatty acyl chains, whereas rat LCAT is more active with PC substrates containing *sn*-2 20:4 (*14*, *15*, *28*, *29*). In a previous study, we identified amino acid residue 149 as responsible for conferring the fatty acyl specificity difference between primates and rodents (*16*). Thus, mutating amino acid 149 from glutamic acid, which is present in human LCAT, to alanine, which is present at position 149 in rat LCAT, resulted in an increased PLA_2 activity and cholesterol esterification with PAPC compared to POPC. In the present study, we explored the molecular basis for our previous observations. Three new findings in the present study help to clarify the influence of this region of LCAT on activity and substrate specificity. First, we observed that the corresponding reverse mutation in rat LCAT (rA149E) resulted in a substrate reactivity profile similar to that of human LCAT for both PLA_2 activity and cholesterol esterification, with reduced activity toward PAPC compared to POPC (Figure 1). This finding suggested that the region around amino acid 149 is critical in conferring substrate specificity of the enzyme, since the impact on activity of substitutions at this amino acid was reversible and context independent. Second, the increased activity of the hE149A LCAT was selective for 20-carbon, but not 18-carbon, chain lengths and was due to an increase in the apparent V_{max} of the enzyme, with little effect on the apparent K_m or surface binding of LCAT to rHDL. Finally, removal of the negative charge at amino acid 149 is necessary to increase the activity of the enzyme with PC substrates containing 20-carbon *sn*-2 fatty acyl chains. We are unaware of any other example of an enzyme in which a single amino acid alters PLA_2 substrate specificity so markedly.

Although the crystal structure of LCAT is unknown, Peelman et al. (*18*) have published a proposed model of LCAT based on the crystal structure of several lipases, including human pancreatic lipase and *Candida antarctica* lipase. LCAT is in the α/β hydrolase fold family, and the Peelman model predicts that the central domain of LCAT consists of seven conserved β strands connected by four α-helices and loops with the catalytic triad at S181, D345, and H377. Amino acid 149 is present in a flexible, hydrophilic loop between the β4 strand and the α4−5 helix. Although there is an 87% amino acid identity between human and rat LCAT, the two enzymes have distinctly different

Table 2: Kinetic Constants for E149 Mutants with rHDL Containing POPC or PAPC[a]

amino acid at position 149	PAPC app V_{max} (nmol of CE h^{-1} μg^{-1})	PAPC K_m (μM Chol)	POPC app V_{max} (nmol of CE h^{-1} μg^{-1})	POPC K_m (μM Chol)	app V_{max} ratio PAPC/POPC
E (WT)	23.85 ± 1.40	1.01 ± 0.18	37.25 ± 1.88	1.37 ± 0.19	0.64
D	23.18 ± 1.34	0.68 ± 0.14	35.53 ± 1.68	1.10 ± 0.16	0.65
Q	17.97 ± 0.86	0.88 ± 0.14	10.28 ± 0.56	0.84 ± 0.15	1.75
A	31.26 ± 1.60	0.59 ± 0.11	24.40 ± 1.11	0.76 ± 0.12	1.28
L	35.85 ± 1.90	0.53 ± 0.11	28.29 ± 1.36	0.71 ± 0.12	1.27
K	6.69 ± 0.31	0.70 ± 0.11	4.73 ± 0.24	0.78 ± 0.13	1.41

[a] See Table 1 legend for experimental details. Kinetic constants for substrate saturation curves were expressed as estimated parameter ± standard error, which was determined by nonlinear regression analysis using the single rectangular hyperbole function in Sigma Plot (Jandel Scientific). WT = wild type.

substrate specificities, as mentioned above. In our previous study, we converted the substrate specificity and reactivity of the human enzyme to those of the rat enzyme by mutating glutamic acid 149 to alanine. In the present study, we reasoned that if this amino acid was critical in determining PC substrate specificity, then the mutation should be independent of the protein background and, thus, the reverse mutation in rat LCAT should convert the substrate specificity of rat LCAT to that of human LCAT. This was indeed the outcome and suggests that amino acid 149 is a critical determinant of enzyme activity with different PC substrates.

The importance of amino acid 149 in determining PC substrate specificity was monitored by using two PC species, POPC and PAPC, which only differed in the *sn*-2 fatty acyl chain. Published studies have indicated that LCAT activity is primarily controlled by the substrate PC it encounters, and the activity is markedly affected by the PC *sn*-2 fatty acyl chain (*8*−*10*). To determine whether the activity difference between hLCAT and hE149A was only apparent with POPC and PAPC or was related to a more general property of PC substrate molecules, we performed studies with PC species that varied in *sn*-2 fatty acyl chain length, number of double bonds, and position and type (cis vs trans) of double bonds. Both enzymes demonstrated a wide range of activities with the various PC substrates containing 18- and 20-carbon *sn*-2 fatty acyl chains as expected (Figure 2). However, there was no discrimination among the *sn*-2 18-carbon PC species for hLCAT and hE149A, whereas the latter enzyme showed consistently higher activity with 20-carbon *sn*-2 fatty acyl chains. This experiment demonstrated that residue 149 of LCAT is important in discriminating *sn*-2 fatty acyl chain length but was not particularly sensitive to differences in the number, type, or position of double bonds along the *sn*-2 fatty acyl chain. As suggested by the proposed structural model of LCAT from Peelman et al. (*18*), mutation of E149 to A may open up the flexible loop around the active site binding pocket, allowing PC molecules with longer *sn*-2 fatty acyl chain to bind more efficiently.

The LCAT reaction consists of multiple steps prior to hydrolysis of the *sn*-2 fatty acyl chain of PC. These include binding of the enzyme to the surface of the lipoprotein particle, activation of the enzyme by apoA-I, and binding of the PC molecule to the active site of the enzyme. Possible molecular explanations for increased reactivity of hE149A with PC molecules containing *sn*-2 20-carbon fatty acyl chains could be an increased binding of the enzyme to the lipoprotein substrate particle surface or an increased binding of PC substrate molecules to the active site. Our LCAT binding assay suggested that rHDL surface binding affinity and capacity, which are represented by K_d and B_{max}, are similar for mutant and wild-type LCAT with both PAPC and POPC rHDL particles (Table 1). This result suggests that the increased reactivity of hE149A is not due to increased rHDL surface binding of the enzyme. By comparing the apparent kinetic constants and dissociation constants from solid-phase binding and activity inhibition assays, Bolin and Jonas (*26*) showed that the apparent K_m for cholesterol esterification of LCAT reflected the binding affinity for the surface of the rHDL particle, whereas the apparent V_{max} reflected a preference of the molecular substrate for the active site. We did not find any significant difference between the apparent K_m values of hE149A and hLCAT, which agreed with the K_d results obtained from direct binding measurements (Table 1). In contrast, the higher apparent V_{max} of hE149A for PAPC compared to hLCAT supports the conclusion that the critical step of LCAT catalysis that is affected by amino acid 149 is the binding of monomeric PC substrate to the active site of LCAT.

To better define the molecular properties of amino acid 149 that determine the *sn*-2 fatty acyl substrate specificity of LCAT, we measured the activity of several mutant forms of LCAT that changed the size, charge, and hydrophobicity of residue 149. All mutant forms of LCAT generated were active, and a range of activities was observed. However, removal of the negative charge on residue 149 was associated with an increased activity with PAPC compared with POPC, whereas the substitution of D for E, which maintained the negative charge, had little effect on overall activity or PC substrate specificity (Figure 4). Helix α4−5, which is C-terminal of the hydrophilic flexible loop containing amino acid 149, is predicted by energy minimization to form a stable lipid-associating helix and is proposed to be involved in PC substrate binding to the active site (*30*). This idea has been supported experimentally by showing that a synthetic helical peptide of this segment (residues 154−171) bound to phospholipids (*30*). In addition, a natural mutation Y156N on the hydrophobic face of helix α4−5, which packs against the hydrophobic side of the central β sheet (*11*), decreasing the hydrophobic moment and lipid-binding capacity of the helix (*30*), caused a 70% reduction on activity (*11*). We propose that the alanine for glutamic acid substitution at position 149 might change the orientation of helix α4−5 to an optimal conformation for interacting with *sn*-2 20-carbon fatty acyl chains by changing the size or shape of the active site pocket. The change in orientation may be accomplished by disrupting a salt bridge between E149 and another residue.

It is interesting to note that two residues, D145 and R147, that are in the same flexible loop as E149 are invariant across 14 species for which the complete sequence of LCAT is known, including *Caenorhabditis elegans*, several species of yeast, *Arabidopsis thaliana*, and *Bacillus licheniformis*. Structural homology of LCAT with human pancreatic lipase has led to the suggestion that D145 and R147 may be involved in a salt bridge that stabilizes the active site pocket of LCAT (*31*). Removal of the negative charge at either of these two residues by site-directed mutagenesis completely destroys the activity of the enzyme, including the esterase activity with a water-soluble substrate (*31*). If E149 does form a salt bridge, its disruption has a strikingly different effect on activity compared to that observed for D145 and R147. Substitution of an uncharged amino acid results in a modest decrease in the activity of the enzyme with POPC but actually increases the activity with PAPC when A or L are the substituted amino acids. Furthermore, only when the positively charged amino acid (K) is substituted for E does overall activity of the enzyme become substantially reduced. These data, taken together, support the hypothesis that E149 is involved in a salt bridge that restricts the size of the active site pocket, resulting in reduced binding efficiency of PC substrates with *sn*-2 20-carbon or longer fatty acyl chains. A corollary to this hypothesis is that breaking the salt bridge by removal of the negative charge at residue 149 results in an increased size of the active site pocket that can better accommodate longer chain (>18-carbon) *sn*-2 fatty acyl chains. Furthermore, introduction of a positive charge at residue 149 may result in a restriction of the active site by formation of another salt bridge or a conformational change that results in low activity with all PC substrates.

To determine whether in vivo expression of hE149A impacts the CE fatty acid composition of plasma lipoproteins, we compared the fatty acyl composition of CEs in plasma HDL of transgenic mice with 20-fold overexpression of hE149A or hLCAT (*32*). The overexpression of hE149A compared to hLCAT significantly enriched HDL with CE species containing 20:4 (45% increase) and 22:6 $n - 3$ (108% increase), at the expense of those containing 18:2, without a significant change in plasma HDL concentration, particle size, or phospholipid fatty acyl composition. Removing the contribution of endogenous mouse LCAT by crossing the transgenic mice into the mouse LCAT knockout background resulted in even greater changes in HDL CE composition, with 2.4-, 5-, and 5-fold increases in 20:4, 20:5 $n - 3$, and 22:6 $n - 3$ CEs, respectively, in hE149A mice compared to hLCAT mice. Previous studies have shown that enrichment of plasma CEs with polyunsaturated species is associated with less atherosclerosis in humans (*33*, *34*), nonhuman primates (*35*−*37*), and mice (*38*). Given the significant enrichment of plasma CEs with polyunsaturated fatty acids in the hE149A mice, we hypothesize that transgenic expression of this mutant form of LCAT compared to wild-type LCAT may reduce atherosclerosis extent. This hypothesis is currently being tested in our laboratory.

ACKNOWLEDGMENT

We gratefully acknowledge the support of the Circular Dichroism Core Laboratory by the North Carolina Biotechnology Center.

REFERENCES

1. Jonas, A. (1998) Regulation of lecithin cholesterol acyltransferase activity, *Prog. Lipid Res. 37*, 209−234.
2. Glomset, J. A., Janssen, E. T., Kennedy, R., and Dobbins, J. (1966) Role of plasma lecithin:cholesterol acyltransferase in the metabolism of high-density lipoproteins, *J. Lipid Res. 7*, 638−648.
3. Glomset, J. A. (1968) The plasma lecithin:cholesterol acyltransferase reaction, *J. Lipid Res. 9*, 155−167.
4. Fielding, C. J., Shore, V. G., and Fielding, P. E. (1972) A protein cofactor of lecithin:cholesterol acyltransferase, *Biochem. Biophys. Res. Commun. 46*, 1493−1498.
5. Fielding, C. J., and Fielding, P. E. (1995) Molecular physiology of reverse cholesterol transport, *J. Lipid Res. 36*, 211−228.
6. Hamilton, R. L., Williams, M. C., Fielding, C. J., and Havel, R. J. (1976) Discoidal bilayer structure of nascent high-density lipoproteins from perfused rat liver, *J. Clin. Invest. 58*, 667−680.
7. Babiak, J., Tamachi, H., Johnson, F. L., Parks, J. S., and Rudel, L. L. (1986) Lecithin:cholesterol acyltransferase-induced modifications of liver perfusate discoidal high-density lipoproteins from African green monkeys, *J. Lipid Res. 27*, 1304−1317.
8. Jonas, A., Zorich, N. L., Kezdy, K. E., and Trick, W. E. (1987) Reaction of discoidal complexes of apolipoprotein A-I and various phosphatidylcholines with lecithin cholesterol acyltransferase. Interfacial effects, *J. Biol. Chem. 262*, 3969−3974.
9. Pownall, H. J., Pao, Q., and Massey, J. B. (1985) Acyl chain and headgroup specificity of human plasma lecithin:cholesterol acyltransferase. Separation of matrix and molecular specificities, *J. Biol. Chem. 260*, 2146−2152.
10. Parks, J. S., Huggins, K. W., Gebre, A. K., and Burleson, E. R. (2000) Phosphatidylcholine fluidity and structure affect lecithin: cholesterol acyltransferase activity, *J. Lipid Res. 41*, 546−553.
11. Peelman, F., Verschelde, J. L., Vanloo, B., Ampe, C., Labeur, C., Tavernier, J., Vandekerckhove, J., and Rosseneu, M. (1999) Effects of natural mutations in lecithin:cholesterol acyltransferase on the enzyme structure and activity, *J. Lipid Res. 40*, 59−69.
12. Portman, O. W., and Sugano, M. (1964) Factors influencing the level and fatty acid specificity of the cholesterol esterification activity in human plasma, *Arch. Biochem. Biophys. 105*, 532−540.
13. Sgoutas, D. S. (1972) Fatty acid specificity of plasma phosphatidylcholine:cholesterol acyltransferase, *Biochemistry 11*, 293−296.
14. Grove, D., and Pownall, H. J. (1991) Comparative specificity of plasma lecithin:cholesterol acyltransferase from 10 animal species, *Lipids 26*, 416−420.
15. Liu, M., Bagdade, J. D., and Subbaiah, P. V. (1995) Specificity of lecithin:cholesterol acyltransferase and atherogenic risk: Comparative studies on the plasma composition and in vitro synthesis of cholesteryl esters in 14 vertebrate species, *J. Lipid Res. 36*, 1813−1824.
16. Wang, J., Gebre, A. K., Anderson, R. A., and Parks, J. S. (1997) Amino acid residue 149 of lecithin:cholesterol acyltransferase determines phospholipase A_2 and transacylase fatty acyl specificity, *J. Biol. Chem. 272*, 280−286.
17. Parks, J. S., Bullock, B. C., and Rudel, L. L. (1989) The reactivity of plasma phospholipids with lecithin:cholesterol acyltransferase is decreased in fish oil-fed monkeys, *J. Biol. Chem. 264*, 2545−2551.
18. Peelman, F., Vinaimont, N., Verhee, A., Vanloo, B., Verschelde, J. L., Labeur, C., Seguret-Mace, S., Duverger, N., Hutchinson, G., Vandekerckhove, J., Tavernier, J., and Rosseneu, M. (1998) A proposed architecture for lecithin cholesterol acyl transferase (LCAT): Identification of the catalytic triad and molecular modeling, *Protein Sci. 7*, 587−599.
19. Wang, J., Gebre, A. K., Anderson, R. A., and Parks, J. S. (1997) Cloning and in vitro expression of rat lecithin:cholesterol acyltransferase, *Biochim. Biophys. Acta 1346*, 207−211.
20. Chisholm, J. W., Gebre, A. K., and Parks, J. S. (1999) Characterization of C-terminal histidine tagged human recombinant lecithin:cholesterol acyltransferase, *J. Lipid Res. 40*, 1512−1519.
21. Huggins, K. W., Curtiss, L. K., Gebre, A. K., and Parks, J. S. (1998) Effect of long chain polyunsaturated fatty acids in the *sn*-2 position of phosphatidylcholine on the interaction with recombinant high-density lipoprotein apolipoprotein A-I, *J. Lipid Res. 39*, 2423−2431.
22. Bohm, G., Muhr, R., and Jaenicke, R. (1992) Quantitative-analysis of protein far UV circular-dichroism spectra by neural networks, *Protein Eng. 5*, 191−195.

23. Parks, J. S., and Gebre, A. K. (1997) Long chain polyunsaturated fatty acids in the *sn*-2 position of phosphatidylcholine decrease the stability of recombinant high-density lipoprotein apoA-I and the activation energy of lecithin:cholesterol acyltransferase reaction, *J. Lipid Res. 38*, 266−275.
24. Parks, J. S., Gebre, A. K., and Furbee, J. W., Jr. (1998) in *Methods in Molecular Biology* (Doolittle, M., and Reue, K., Eds.) pp 123−131, Humana Press, Totowa, NJ.
25. Green, N. M., Konieczny, L., Toms, E. J., and Valentine, R. C. (1971) The use of bifunctional biotinyl compounds to determine the arrangement of subunits in avidin, *Biochem. J. 125*, 781−791.
26. Bolin, D. J., and Jonas, A. (1994) Binding of lecithin:cholesterol acyltransferase to reconstituted high-density lipoproteins is affected by their lipid but not apolipoprotein composition, *J. Biol. Chem. 269*, 7429−7434.
27. Jin, L. H., Lee, Y. P., and Jonas, A. (1997) Biochemical and biophysical characterization of human recombinant lecithin: cholesterol acyltransferase, *J. Lipid Res. 38*, 1085−1093.
28. Pownall, H. J., Pao, Q., and Massey, J. B. (1985) Isolation and specificity of rat lecithin:cholesterol acyltransferase: comparison with the human enzyme using reassembled high-density lipoproteins containing ether analogs of phosphatidylcholine, *Biochim. Biophys. Acta 833*, 456−462.
29. Hida, Y., Furukawa, Y., Urano, T., Kim, H. J., and Kimura, S. (1993) Substrate specificity of rat plasma lecithin-cholesterol acyltransferase towards a molecular species of phosphatidylcholine, *Biosci., Biotechnol. Biochem. 57*, 1111−1114.
30. Peelman, F., Goethals, M., Vanloo, B., Labeur, C., Brasseur, R., Vandekerckhove, J., and Rosseneu, M. (1997) Structural and functional properties of the 154−171 wild-type and variant peptides of human lecithin-cholesterol acyltransferase, *Eur. J. Biochem. 249*, 708−715.
31. Peelman, F., Vanloo, B., Verschelde, J. L., Labeur, C., Caster, H., Taveirne, J., Verhee, A., Duverger, N., Vandekerckhove, J., Tavernier, J., and Rosseneu, M. (2001) Effect of mutations of N- and C-terminal charged residues on the activity of LCAT, *J. Lipid Res. 42*, 471−479.
32. Furbee, J. W., Jr., Francone, O. L., and Parks, J. S. (2001) Alteration of plasma HDL cholesteryl ester composition with transgenic expression of a point mutation (E149A) of human lecithin:cholesterol acyltransferase (LCAT), *J. Lipid Res. 42*, 1626−1635.
33. Kingsbury, K. J., Brett, C., Stovold, R., Chapman, A., Anderson, J., and Morgan, D. M. (1974) Abnormal fatty acid composition and human atherosclerosis, *Postgraduate Medical Journal 50*, 425−440.
34. Kingsbury, K. J., Stovold, R., Morgan, D. M., and Brett, C. G. (1969) The relationships between plasma cholesteryl polyunsaturated fatty acids, age and atherosclerosis, *Postgrad. Med. J. 45*, 591−601.
35. Parks, J. S., Johnson, F. L., Wilson, M. D., and Rudel, L. L. (1990) Effect of fish oil diet on hepatic lipid metabolism in nonhuman primates: lowering of secretion of hepatic triglyceride but not apoB, *J. Lipid Res. 31*, 455−466.
36. Wolfe, M. S., Sawyer, J. K., Morgan, T. M., Bullock, B. C., and Rudel, L. L. (1994) Dietary polyunsaturated fat decreases coronary artery atherosclerosis in a pediatric-aged population of African green monkeys, *Arterioscler. Thromb. 14*, 587−597.
37. Rudel, L. L., Parks, J. S., and Sawyer, J. K. (1995) Compared with dietary monounsaturated and saturated fat, polyunsaturated fat protects African green monkeys from coronary artery atherosclerosis, *Arterioscler. Thromb. Vasc. Biol. 15*, 2101−2110.
38. Rudel, L. L., Kelley, K., Sawyer, J. K., Shah, R., and Wilson, M. D. (1998) Dietary monounsaturated fatty acids promote aortic atherosclerosis in LDL receptor-null, human ApoB100−Overexpressing transgenic mice, *Arterioscler. Thromb. Vasc. Biol. 18*, 1818−1827.

BI035460U